Wind Measurements from Four Airliners in 1988 Denver Microburst

R. A. Coppenbarger* and R. C. Wingrove*
NASA Ames Research Center, Moffett Field, California 94035

Flight and radar position records are analyzed to determine the winds encountered by four airliners that penetrated a microburst on approach to Denver's Stapleton International Airport on July 11, 1988. The four encounters provide information about the time-varying changes in the strength, size, and location of the microburst phenomenon. The results show significant expansion in the size of the microburst and indicate the presence of fluctuations in the internal wind velocity associated with multiple microburst cells. At its peak strength, as experienced by the second aircraft, the microburst produced a headwind-to-tailwind velocity change of 115 ft/s. It is shown that the developing wind patterns derived from the flight-data analysis are in general agreement with results derived from ground-based Doppler weather radar and from a numerical microburst simulation. The data from the four aircraft complement these other findings by providing a more detailed analysis of the microburst's internal wind environment.

Introduction

LOW-LEVEL microburst windshear is a continuing problem that must be better understood in the interest of aircraft safety.[1-3] In recent years, research efforts have included 1) the development of ground-based systems for the detection of microburst activity, 2) the development of meteorological models to predict microburst flowfields, and 3) the analysis of airline flight records of actual microburst encounters to obtain high-resolution wind estimates along flight paths. Although these efforts have proceeded in parallel, there has been no opportunity to apply each approach to a single windshear event. Additionally, previous analyses of airline flight records have been primarily limited to microburst encounters involving single aircraft, which can only provide wind estimates over short time periods and along single trajectories.

Recently, flight records have become available from four airliners that penetrated a microburst while approaching Denver's Stapleton International Airport on the afternoon of July 11, 1988. In addition to making multiple flight records available, this incident was unique because of the presence of Doppler weather radar that was being evaluated at Denver at the time of the incident. Meteorological soundings were also available before the incident, and they were later used as initial conditions for an advanced flowfield simulation of the microburst.

The aircraft involved, shown in Fig. 1, were short- and medium-range jet transports that were making visual approaches from the east. After encountering the microburst east of the runway threshold, all four aircraft aborted their approaches and initiated go-arounds.[4] Despite the strength of the microburst, there were no injuries to those aboard the airliners and no damage to the aircraft.

During the summer of 1988, two Doppler weather radar systems were in operation near Stapleton airport as part of a test and demonstration project to detect windshear in the terminal area.[5] Wind-velocity fields obtained from both single- and dual-Doppler scans were provided[6] to allow comparison with winds derived through analysis of flight data. Measurements from surface wind sensors, situated in the vicinity of the approach paths, were also available.

Denver weather soundings, taken about one hour before the aircraft encounters with the microburst, were used to provide initial conditions for an advanced microburst flowfield model.[7] This model provided an additional three-dimensional prediction of microburst winds.[8]

The purpose of this paper is to present relevant wind information derived from the onboard flight records and compare it with data from the ground-based Doppler radar, surface wind sensors, and the advanced numerical model. Through this analysis, a detailed history of the structure and development of the microburst is produced. Large-scale characteristics, such as size, shape, and cell locations are estimated from the Doppler data, whereas small-scale characteristics, such as internal turbulence and peak wind velocities, are obtained from the aircraft flight data.

The paper first describes the procedure used to calculate wind velocity from the flight data. The aircraft trajectories are then discussed, and results are presented that show the important physical characteristics of the microburst. Finally, flight-path winds are compared with those obtained from the Doppler radar, surface wind sensors, and the numerical simulation.

Method of Analysis

The aircraft data included both air traffic control (ATC) radar position data and foil flight-recorder data. The radar data, recorded every 4.7 s, included range, azimuth, and mode-C transponded pressure altitude. The inertial coordinates of each aircraft were reconstructed in a Cartesian frame (x,y,h) with its origin at the threshold of runway 26L at Stapleton. The radar data were smoothed to reconstruct inertial velocities, which typically change slowly even in the presence of atmospheric disturbances. The flight data, recorded continuously on a metal foil medium, included pressure altitude, indicated airspeed, heading, and normal acceleration. The two data sets were synchronized through a time-history comparison of the onboard recorded altitude and the ATC-transponded altitude.

Because of the limited number of parameters recorded, vertical winds were not determined, and it was necessary to calculate horizontal winds using specialized solutions (devel-

Received Aug. 10, 1987; presented as Paper 89-3354 at the AIAA Atmospheric Flight Mechanics Conference, Boston, MA, August 14-16, 1989; revision received March 19, 1990; accepted for publication March 24, 1990.

*Aerospace Engineer. Member AIAA.

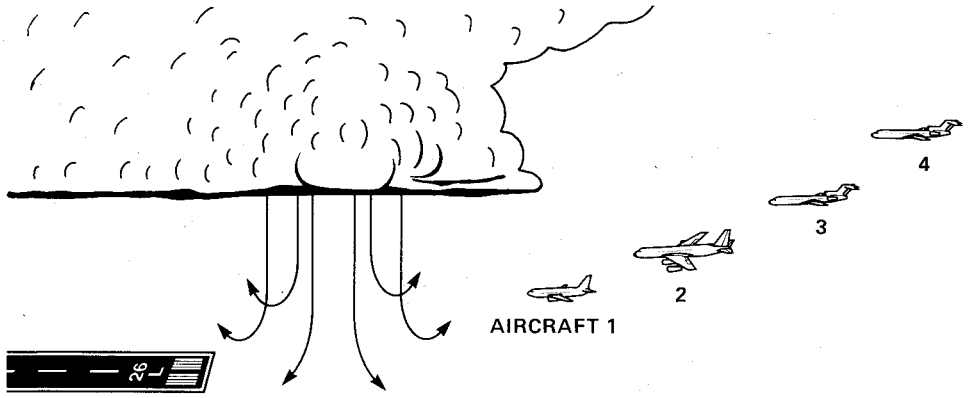

Fig. 1 Overview of the Denver microburst of July 11, 1988.

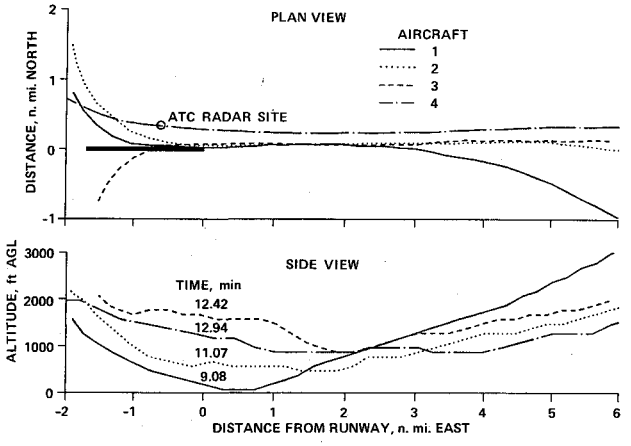

Fig. 2 Trajectories for four airliners.

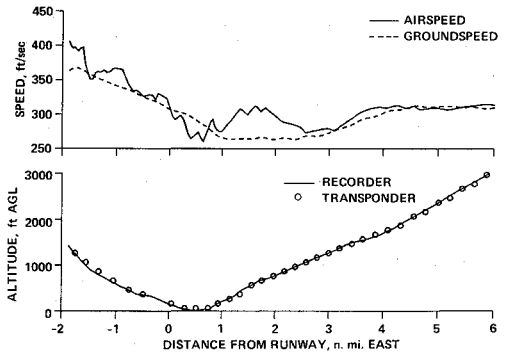

Fig. 3 Speeds and altitude for aircraft 1.

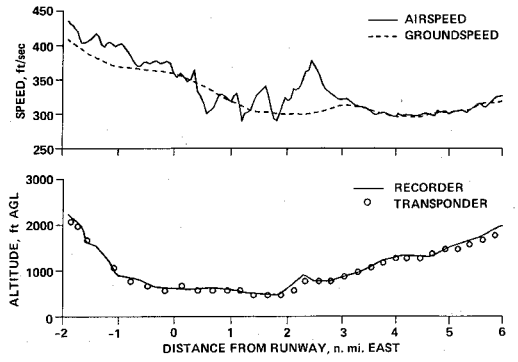

Fig. 4 Speeds and altitude for aircraft 2.

oped in Ref. 9) as follows. The winds along the aircraft flight path are calculated from

$$W_{fp} = V_i - V_a \tag{1}$$

where the inertial ground speed V_i is given by

$$V_i = \sqrt{\dot{x}^2 + \dot{y}^2}$$

The inertial ground speed is derived from the ATC radar data, and the true airspeed V_a is determined from the flight data. Equation (1) applies when the flight-path angle is small and also when the difference between the ground-axis heading angle and the wind-axis heading angle is small. This is a very robust solution and applies well along the trajectories considered in this report.

The horizontal wind components are determined as

$$W_x = \dot{x} - V_a \cos\Psi_a$$
$$W_y = \dot{y} - V_a \sin\Psi_a \tag{2}$$

where x and y are positive toward the north and east, respectively. The heading angle Ψ_a is measured from the aircraft gyro and obtained from the foil data. This solution applies under the same flight conditions noted for Eq. (1) but is more restrictive since it requires further conditions wherein the roll and sideslip angles are small. These conditions are generally met during the stabilized final approach but do not hold after the aircraft starts a turn, typically over the approach end of the runway in a go-around maneuver.

Results and Discussion

Aircraft Trajectories and Speeds

The trajectories of the four aircraft, reconstructed from the ATC radar data, are shown in Fig. 2. The upper plot in Fig. 2 shows a plan view (x,y), and the lower plot shows a side view (h,y). The approximate times at which each aircraft passed over the runway threshold are also indicated in Fig. 2 (in minutes after 2200 GMT). Speed and altitude profiles for each aircraft, presented as functions of distance from the threshold of runway 26L, are shown in Figs. 3–6. In each of these figures, the upper plot shows the true airspeed V_a and the inertial ground speed V_i. The differences between these two curves are the winds encountered along the aircraft flight paths. The lower plots show the altitude above ground level as determined from both the flight recorder and the ATC transponder.

The microburst winds and subsequent go-around maneuvers, as depicted in Figs. 3–6, are discussed separately below for each of the four aircraft.

Aircraft 1

At approximately 2.5 n.mi. east of runway 26L, the first aircraft began experiencing an increasing headwind (differ-

ence between airspeed and ground speed), indicating its initial encounter with the microburst (Fig. 3). The headwind increased to 40 ft/s and then began decreasing, eventually transitioning to a peak tailwind of 30 ft/s. Thus, the resulting headwind-to-tailwind change ΔV was 70 ft/s and occurred over a 25-s period.

Comments from the crew made after the incident indicate that the airplane was initially flown at a higher than normal airspeed and above the glide slope in anticipation of windshear conditions. At about 1 n.mi. from the runway, a ground-proximity warning sounded and the crew, observing that the airspeed had also begun to decrease rapidly, applied takeoff thrust and rotated the airplane to takeoff pitch attitude. The onset of light rain was noted at this point, the flaps were reduced, and the landing gear was raised. During the rest of the go-around, only light turbulence was observed. The flight data show that the airplane was less than 100 ft above the ground at its minimum altitude, near the center of the microburst. The crew noted that upon the addition of thrust, the aircraft continued to lose altitude for a short period after which both airspeed and altitude increased simultaneously and the aircraft recovered normally.

Aircraft 2

The results show that the second aircraft encountered a head wind at about 2.8 n.mi. from the threshold that increased rapidly to 80 ft/s (Fig. 4). The headwind then decreased to a tailwind of 10 ft/s within a 15-s period. During the next 25 s, fluctuations in wind velocity were experienced before a peak tailwind of 35 ft/s was reached. The resulting ΔV, 115 ft/s occurring within 35 s, was the largest of all four aircraft.

The crew, aware of possible wind-shear conditions in the area, maintained an airspeed that was 10 kt greater than normal for the approach. On entering the microburst, the airspeed suddenly increased and thrust was reduced. At idle thrust, the crew noted that the aircraft appeared to be riding on a smooth wave with increasing airspeed. Anticipating a sudden loss in airspeed, full power was applied. During the recovery, moderate turbulence was encountered with violent jolts that appeared to move the airplane vertically and laterally. The crew noted that the aircraft climbed very slowly at first, despite takeoff power and a nose-up pitch attitude. The flight data show that the go-around was initiated at about 2 n.mi. east of runway 26L. During the subsequent recovery, the data show that the airplane remained near a constant altitude of 700 ft, although its airspeed increased markedly.

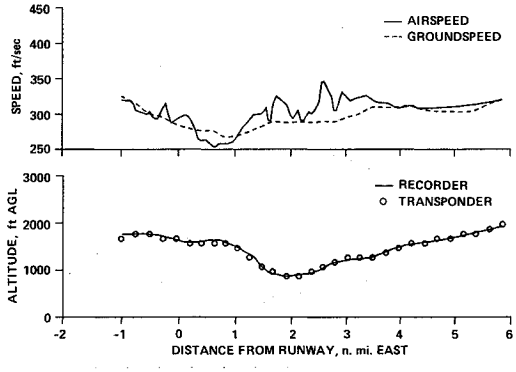

Fig. 5 Speeds and altitude for aircraft 3.

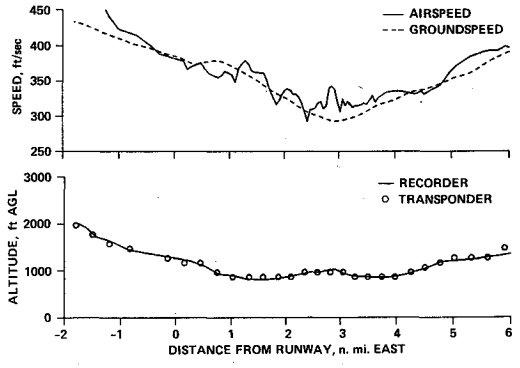

Fig. 6 Speeds and altitude for aircraft 4.

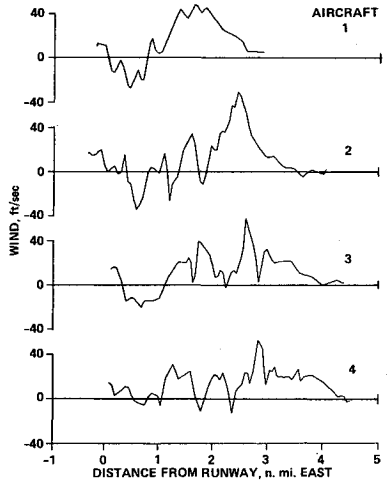

Fig. 7 Winds along the flight paths for four airliners.

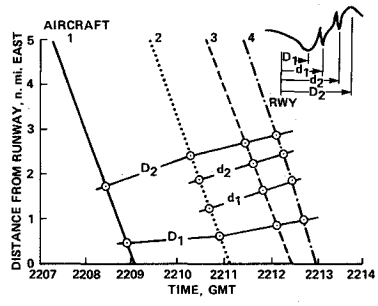

Fig. 8 Time variation of microburst location.

Aircraft 3

The third aircraft encountered an increasing headwind at about 3.5 n.mi. from the runway threshold (Fig. 5). This headwind increased to 60 ft/s over a distance of 1 n.mi. and was followed by wind-velocity fluctuations similar to those experienced by the previous aircraft. The aircraft encountered a maximum tailwind of 20 ft/s, resulting in a ΔV of 80 ft/s within a 45-s period.

The crew, flying the aircraft faster and higher than normal, observed an increase in airspeed at the leading edge of the microburst. The aircraft, as it encountered the downdraft, experienced a strong shock accompanied by a sudden loss in airspeed. In response, full power was applied, and the airplane was rotated and held at a pitch angle of 15 deg—in accordance with standard wind-shear recovery procedure.[3] The flight data show that the go-around was initiated at an altitude of about 900 ft, with a sharp pull-up leading to a subsequent gain in altitude to approximately 1700 ft. Figure 5 shows that airspeed was traded for altitude during the initial part of the go-around.

Aircraft 4

The data in Fig. 6 show that the fourth aircraft experienced the least severe windshear, with a maximum headwind of 45 ft/s that eventually transitioned into a tailwind of 25 ft/s. This resulted in a ΔV of 65 ft/s within 40 s. The aircraft also

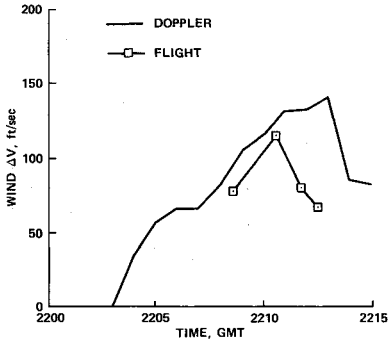

Fig. 9 Maximum ΔV along flight paths compared with those from TDWR.

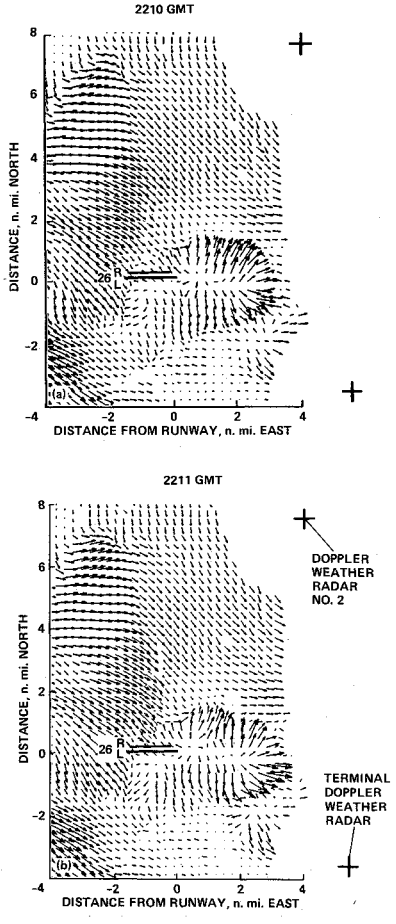

Fig. 10 Location of Doppler radar sites and derived wind pattern at two times.

experienced significant wind-velocity oscillations within the core of the microburst, as did the previous two aircraft.

After experiencing difficulty in slowing the aircraft for the approach and hearing the prediction of an 80-kt loss by air traffic control, the crew executed a standard go-around procedure. During the go-around, moderate turbulence was encountered, and the aircraft did not achieve its expected climb performance. Similar to the second aircraft, this aircraft remained at nearly constant altitude (between 900 and 1,100 ft) while traversing the microburst, during which time its airspeed increased.

Microburst Development and Structure

Figure 7 presents a comparison of the flight-path winds for the four aircraft. As indicated in the above discussion, the most intense windshear was experienced by the second aircraft. The wind profiles suggest that the microburst activity was expanding during the successive encounters. The distance between velocity peaks (maximum headwind and tailwind) was about 1.3 n.mi. at the time of the first aircraft encounter and grew to over 2 n.mi. by the time of the fourth aircraft encounter. Of greatest significance is the finding of the oscillatory winds that developed between the time that the first and second aircraft traversed the microburst. In comparing the wind profiles of the last three aircraft (Fig. 7), these velocity fluctuations show a similar pattern, with peaks spaced about 0.4 n.mi. apart and occurring near the center of the microburst. Parameters describing the occurrence of these fluctuations are shown in Fig. 8.

Figure 8 shows the primary features of the wind profiles evident in Fig. 7 plotted in temporal and spatial coordinates for each aircraft. The positions, with respect to the runway threshold, of maximum tail and head winds for each encounter are designated by D_1 and D_2, respectively. Internal peak tail winds, describing the fluctuations observed for the second, third, and fourth aircraft, are designated by d_1 and d_2.

Comparisons

In Fig. 9, the maximum ΔV encountered by the four airplanes is compared with the maximum ΔV measured by a single terminal Doppler weather radar (TDWR).[6] As can be seen, the maximum ΔV from the flight data is somewhat below those measured by the radar. This is to be expected, since the maximum ΔV reported by Doppler radar is the maximum seen in any one direction. Data, presented later in

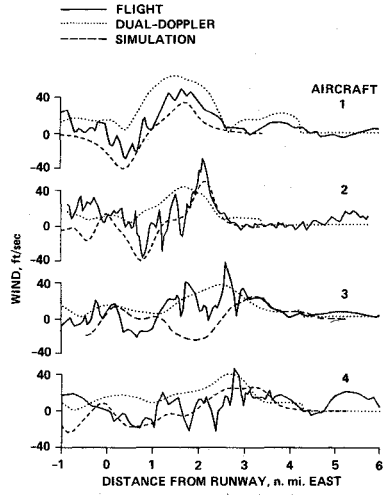

Fig. 11 Winds along the flight paths compared with winds from dual-Doppler and numerical simulation.

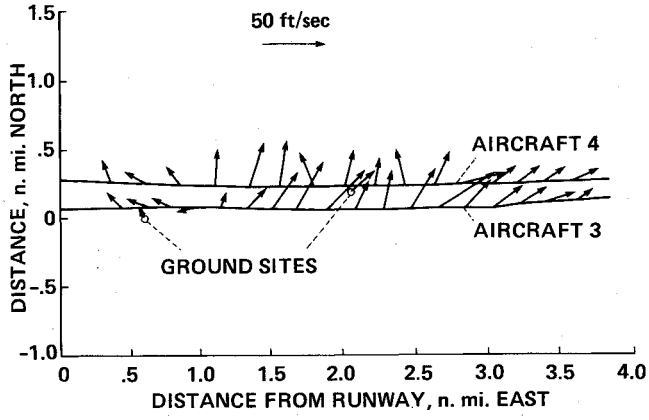

Fig. 12 Wind vectors from two airliners compared with those measured at two surface sites.

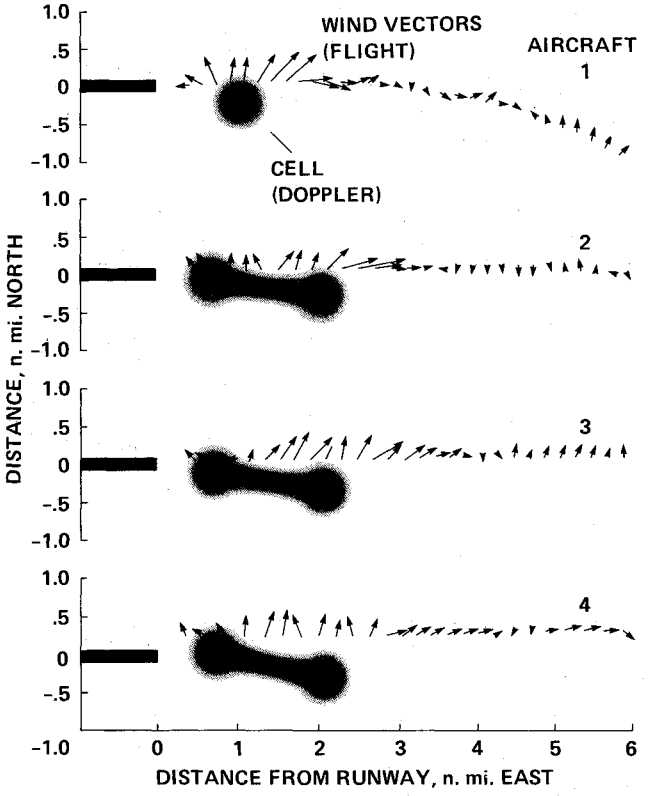

Fig. 13 Wind vectors from four airliners compared with microburst cells from dual Doppler.

the report, indicate that the airplanes did not penetrate the center of the microburst cell(s) and thus did not encounter maximum wind changes.

With a single Doppler radar, only the radial component of the wind velocity can be measured. To provide both components of the wind vectors, data from the additional Doppler radar site were utilized. The location of the two radar sites with respect to the runways at Stapleton is shown in Fig. 10. Flight-path winds resulting from the dual-Doppler analysis are shown in comparison with those derived from the flight records in Fig. 11. Since the minimum spatial resolution of the Doppler data is 820 ft in the horizontal plane and 1640 ft in the vertical axis, the Doppler-derived winds are naturally more smoothed than those derived from the flight data. Additional filtering results from the combination of data from the two Doppler radars and from the conversion from spherical to Cartesian coordinates. Because of the smoothing involved and low spatial resolution, the Doppler data do not resolve subtle wind phenomena such as the velocity fluctuations mentioned earlier. Furthermore, the temporal resolution of the Doppler data used in plotting Fig. 11 was very low, with data available only at 2.5-min intervals. These considerations help explain the discrepancies between the Doppler wind estimates and those derived from the flight data. Figure 11 also shows the flight-path winds predicted by the numerical simulation.[7] Because of low resolution, this model (like the Doppler data) does not show the internal wind fluctuations present in the flight data.

The lowest altitude at which the Doppler-derived winds were available was approximately 600 ft above ground level. To obtain a comparison of flight-path winds at a lower altitude, data from two surface wind sensors were also compared with the flight data. In Fig. 12, the winds measured by the ground sensors[6] are compared with winds encountered by the third and fourth aircraft. These two aircraft traversed the microburst at close time intervals but with different trajectories. The fourth aircraft, which was approaching 26R, was about 0.25 n.mi. north of the third aircraft, which was approaching 26L. As shown, the flight-data-derived winds agree closely with those from the ground sites in both direction and magnitude.

Comparison of the dual-Doppler data, shown in Figs. 10a and 10b at times 2210 and 2211, suggests that the microburst activity initially involved a single cell with a second cell appearing later, aligning with the first in the east-west direction.[6] The microburst cells described here refer to distinct regions of outflow wind and should not be confused with the parental thunderstorm cells. Both Doppler data and flight data indicate that the second microburst cell reached the surface some time between the passage of the first and second aircraft. In Fig. 13, horizontal wind vectors, measured by the aircraft, are shown in comparison with the cell locations (depicted by circles). These cell locations were construed from the dual-Doppler data.

The pattern of the winds encountered are shown to be dependent on the track of each aircraft with respect to the cells. The first aircraft encountered a cell with a center located to the south of its track. With two cells developing near the approach path, the second airplane encountered the edge of the eastern cell and proceeded to penetrate the center of the cell closest to the runway. By the time the third aircraft approached, the two cells had drifted slightly in a southeasterly direction. The third airplane passed through the northern section of the outermost cell and proceeded to pass just north of the center of the innermost cell. The trajectory of the fourth aircraft passed well to the north of the center of both microburst cells. Note that the aircraft was approaching 26R and, thus, had a track farther north than the previous three aircraft.

Concluding Remarks

From the resulting wind profiles it is evident that the four aircraft encountered very strong microburst activity, with a peak headwind-to-tailwind velocity change of 115 ft/s. Since records from multiple aircraft were available, the time-history development of the microburst phenomenon was evident. Because of the appearance of the secondary cell, the extent of the microburst activity (distance between wind-velocity peaks) in the east-west direction grew from 1.3 to 2 n.mi. A significant result of this analysis is the finding of velocity fluctuations developing within the microburst boundaries. The results for the last three aircraft show that these internal fluctuations exhibited a similar pattern, with peaks spaced about 0.4 n.mi. apart. The developing wind pattern measured from the aircraft is in general agreement with the measurements from the Doppler radar and with the analytical results from the numerical model. The aircraft data complement these other findings by providing a detailed analysis of the internal velocity fluctuations. The Doppler data, in particular, add insight by suggesting the presence of a secondary microburst cell. It is very possible that the combined outflows from the two adjacent microburst cells were responsible for most of the turbulent oscillations in horizontal winds observed in the flight data of the latter three aircraft. Investigation into the multicell microburst phenomenon and its effect on the performance and recovery ability of an aircraft are subjects for further research.

Acknowledgments

The flight records and air traffic control radar data used in this investigation were provided by the National Transportation Safety Board. The Doppler radar data were obtained through the National Center for Atmospheric Research (NCAR). The Doppler radar sites were in operation at Stapleton as part of a test and demonstration project, sponsored by the Federal Aviation Administration, to detect windshear in the terminal area. The project was carried out as a joint effort between NCAR and the Massachusetts Institute of

Technology Lincoln Laboratory. The secondary Doppler radar was operated by the University of North Dakota. The microburst model used for comparison in this investigation was the Terminal Area Simulation System model developed through the support of NASA Langley Research Center.

References

[1]*Low-altitude Windshear and Its Hazard to Aviation*, National Academy of Sciences, National Academy, Washington, DC, 1983.

[2]Fujita, T. T., "The Downburst," Satellite and Mesometeorology Research Project, SMRP Research Paper 210, Univ. of Chicago, Chicago, IL, 1985.

[3]"Windshear Training Aid," Federal Aviation Administration, Washington, DC, 1987.

[4]Ireland, B., "Microburst Encounter, July 11, 1988, Denver, Colorado," *Windshear Case Study: Denver, Colorado, 11 July 1988*, Federal Aviation Administration DOT/FAA/DS-89/19, Appendix 1, 1989, pp. 41–120.

[5]"Terminal Doppler Weather Radar Operational Demonstration," Federal Aviation Administration, Washington, DC, 1988.

[6]Elmore, K., Politovich, M., and Sand, W., "Draft Technical Report to the FAA: The 11 July 1988 Microburst at Stapleton International Airport, Denver, CO," *Windshear Case Study: Denver, Colorado, 11 July 1988*, Federal Aviation Administration DOT/FAA/DS-89/19, Appendix 5, 1989.

[7]Proctor, F. H., and Bowels, R. L., "Investigation of the Denver 11 July 1988 Microburst Storm with the Three-Dimensional NASA-Langley Windshear Model," *Windshear Case Study: Denver, Colorado, 11 July 1988*, Federal Aviation Administration DOT/FAA/DS-89/19, Appendix 2, 1989.

[8]Proctor, Fred H., "Numerical Simulations of an Isolated Microburst. Part I: Dynamics and Structure," *Journal of Atmospheric Sciences*, Vol. 45, No. 21, 1988, pp. 3139–3160.

[9]Bach, R. E., and Wingrove, R. C., "Equations for Determining Aircraft Motions from Accident Data," NASA TM-78609, June 1980.